Building Arrays with the Unidirectional-Radiating Complementary Strip-Slot

Alberto Hernández Escobar, Elena Abdo Sánchez, and Carlos Camacho Peñalosa
{ahe, elenaabdo, ccp}@ic.uma.es
Instituto Universitario de Investigación en Telecomunicación, Escuela Técnica Superior de Ingeniería de Telecomunicación,
Universidad de Málaga, Andalucía Tech, Bulevar Louis Pasteur 35, 29010 Málaga, Spain

***Abstract*—An upgraded version of the complementary strip-slot radiating element is reviewed. The original radiating element consists in a microstrip-fed slot in transmission configuration. In the proposed modification, the slot is backed by a cavity in order to obtain unidirectional radiation. The presence of this cavity changes the behavior of the slot. A new equivalent circuit is used to propose a design methodology for broadband operation. Two array designs are simulated and implemented: a phased array and a log-periodic array. Promising experimental results verify the unidirectional radiation and the wide bandwidth of these antennas.**

I. Introduction

Now more than ever, the world needs to be fully interconnected by digital means. The efforts of the past years have allowed reducing mobility and physical interaction (inevitable some time ago), in addition to increasing the working efficiency of developed countries. However, more work must be done in order to achieve real-time global communications that are accessible to everyone. For this aim, extremely high bitrates are also required in wireless links. Despite the fact that the antenna design in the context of communication systems is one of the most classic challenges in telecommunication engineering, the antennas for new applications and recently-appeared services may require special attention in their development or further research. These enhanced functionalities can include wide bandwidth, high efficiency, high directivity, small size, low cost, and easy integration.

Slot-like radiators [1] have been traditionally strong candidates when designing high-performance small antennas due to their many advantages, such as lightweight, high cross-polarization discrimination, low profile, and low manufacturing cost. Thus, they may be a good solution for the antennas of future communication systems. However, although the bandwidth of these radiators is enough for narrow-band applications, it will be insufficient for more demanding, high-bitrate systems. Slot radiating elements have a very resonant nature which compromises their impedance bandwidth considerably.

In [2], a new radiating element, the so-called ‘complementary strip-slot’ was proposed. It consist in a microstrip-fed slot in transmission configuration. A stub is placed in the feeding line, just beneath the slot. Its special feature is that it has a very broad matching. Additionally, the element is simple, easy to implement, and its design is straightforward. This new element has proven to be a solid radiator for building arrays, such as phased arrays [3] or log-periodic arrays [4]. Microstrip-fed slots, however, radiate towards both half-spaces, since it consists of a slot printed on a single ground plane. This means that there will be at least two main beams when an array made of this element is built. Thus, they can be a poor antenna choice when a single, directional beam is desired since it wastes power on an additional beam.

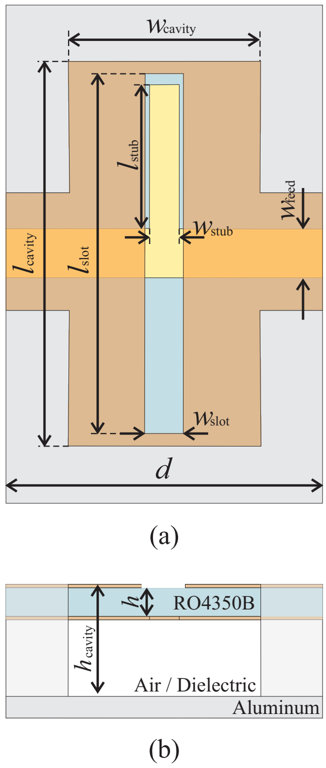

Fig. 1. Geometry of the unit cell of the proposed arrays.

II. The Unidirectional-Radiating Complementary Strip-Slot Element

The problem of the bilateral radiation pattern of the classic complementary strip-slot was tackled by closing the structure. This has been done by changing the microstrip lines for striplines or enclosed microstrips. After this change, a cavity appears underneath the slot and, for this reason, the behavior of the radiating element changes significantly. The structure is shown in Fig. 1. The radiating element consists of a slot transversally fed by a strip printed on a substrate. The substrate is placed on top of an aluminum cavity to form a closed structure. As in the complementary strip-slot, the bandwidth of the radiating element is greatly enhanced by the presence of a stub in the feeding line. A previous version of this radiating element was proposed in [5].

In order to understand the behavior of the radiating element and significantly simplify the design process, a lattice-network ([6]) equivalent circuit has been found. The lattice network is

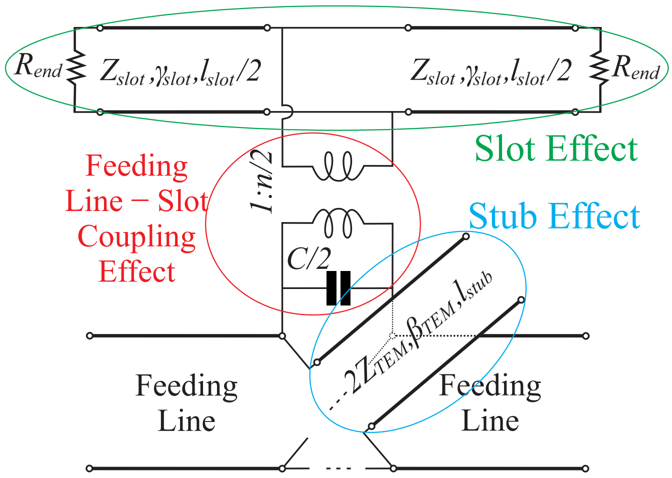

Fig. 2. Lattice network equivalent circuit of the unit cell.

able to separate the effect of the even and odd modes of the structure into its two branches: the parallel branch and the series branch, respectively. For this reason, the effect of the slot (odd mode) will be modeled into the series branch and the effect of the stub (even mode) into the parallel branch. This separation allows designing both elements (slot and stub) separately, which makes the process easier. The behavior of the slot, however, is greatly affected by the presence of the cavity and, thus, to model it, the equivalent circuit proposed in [7] was used. The resulting lattice-network equivalent circuit is shown in Fig. 2. Three different effects can be discerned. First, the effect of the slot, modeled as a transmission line ended in a resistor, which models the radiation losses. The slot mode has cut-off frequency due to the cavity and so must be included in the characteristic impedance and propagation constant of that line. Secondly, the coupling effect between the feeding strip and the slot, which can be controlled by changing the distance between these elements. Finally, the effect of the stub, which can be modeled as a simple transmission line ended in open circuit. Using the impedances of the lattice network (Z_a the impedance of the series branch and Z_b the impedance of the parallel branch), it is possible to express the image impedance of the two-port as a function of frequency as:

$$Z_{im}(\omega) = \sqrt{Z_a(\omega) Z_b(\omega)}. \tag{1}$$

Both the slot and the stub are resonant elements and, thus, by properly choosing the length of the stub, it is possible to almost cancel the pole of Z_a out with the zero of Z_b, obtaining a flat image impedance in a wide bandwidth. The impedance level can be adjusted using the width of the stub or the distance between the feeding line and the slot.

However, in the design of the slot and cavity, it is important to consider the resonance of the TE_{10} mode. This resonance will produce a mismatch, limiting the bandwidth. It can be computed as:

$$f_{101} = \frac{c}{2\sqrt{\mu_r \varepsilon_r}} \sqrt{\frac{1}{w_{cavity}^2} + \frac{1}{l_{cavity}^2}}, \tag{2}$$

where l_{cavity} and w_{cavity} are those shown in Fig. 1. To increase the cut-off frequency of the TE_{10} mode and, thus, a wider working bandwidth, a narrow cavity, with a low w_{cavity}, is preferred. However, if the cavity width, w_{cavity}, is reduced, the cut-off frequency of the slot mode will increase, and the slot will start radiating at a higher frequency. To broaden the operating frequency band, the cut-off frequency of the slot mode can be lowered by increasing the height of the cavity, h_{cavity}. Thus, it is important to reach a compromise between bandwidth and element thickness. Furthermore, w_{cavity} will also limit the distance between the elements of the arrays, which is a very important parameter in their design.

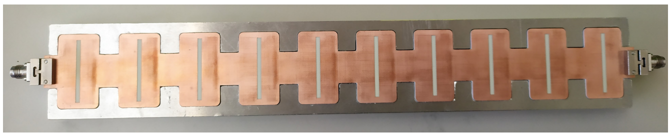

Fig. 3. Picture of the manufactured phased array.

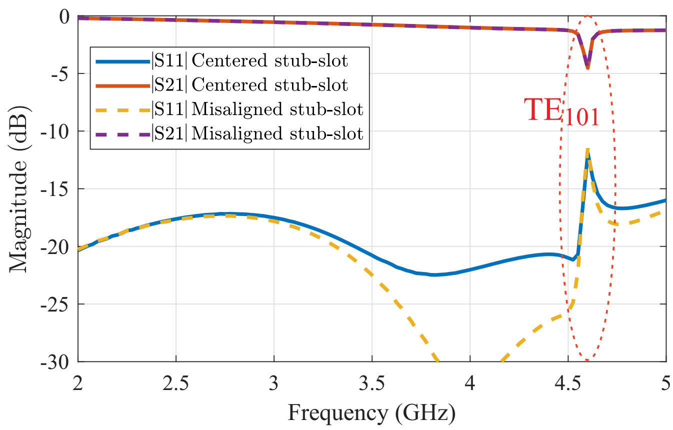

Fig. 4. Magnitude of the S parameters of the unit cell of the phased array with and without misalignment.

III. Series-Fed Arrays

The transmission configuration of this radiating element makes it ideal to build broadband series-fed arrays like these proposed in this section. Two different classic array topologies have been analyzed and manufactured, a phased array and a log-periodic array.

A. Phased Array

A uniform phased array has been built by cascading ten elements, in order to perform frequency scanning. Fig. 3 shows the manufactured prototype. Between the substrate and the aluminum cavity, a layer of 3D-printed dielectric material is placed to hold the substrate. A small misalignment between the strip and slot elements is added to the unit cell in order to reduce the problem of the open stopband at broadside. The degree of freedom of this asymmetry allows obtaining an even lower level of the $|S_{11}|$ parameter. Such a good matching can be obtained so that, even if the reflections are added in phase, there will be less reflected power at the source. Fig. 4 shows the S parameters of the unit cell of the proposed phased array, where it is possible to see that adding the misalignment resulted in an even lower S_{11} parameter from 3.25 GHz onward. It can also be seen the resonance of the resonant mode TE_{101} at 4.6 GHz.

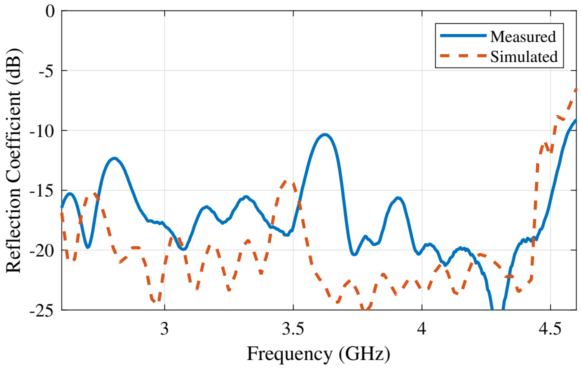

Fig. 5. Reflection coefficient of the proposed phased array.

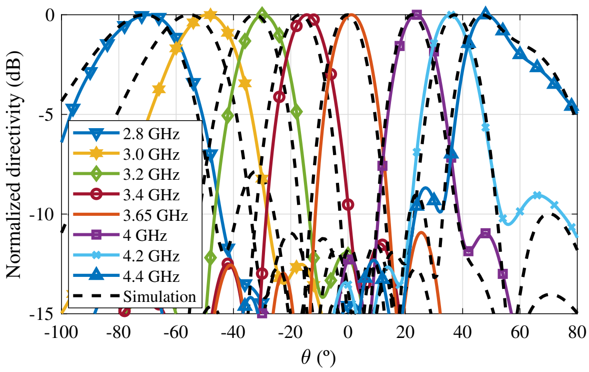

Fig. 6. Radiation patterns of the proposed phased array at different frequencies.

The designed phased array has 10 radiating elements. The power radiated by a single element can be adjusted with the width of the slot. Special attention was paid to the design of the distance between the elements. To maximize the bandwidth of the array, the distance was adjusted so the array pattern finishes scanning at the resonance of the cavity, at 4.6 GHz. The resulting array radiates broadside at 3.65 GHz.

The measured S parameters of the fabricated structure are shown in Fig. 5 together with those from the HFSS simulation. Good matching is obtained in both cases, with return losses higher than 10 dB in the working band. To verify the array scanning capabilities, the measurement of its radiation pattern was carried out. Fig. 6 shows the radiation patterns in the plane longitudinal to the feeding strip (co-pol) obtained for the array at several frequencies in the radiation band. The agreement between simulation and measurement is excellent and, as expected, they demonstrate its scanning behavior. The antenna can continuously scan its beam from -70° to 50°. No significant gain degradation is found at broadside, unlike LWAs without open-stopband suppression. The obtained maximum gain, 11 dB, is reasonable given the size of the array, and is stable in frequency, changing only around 3.5 dB over the whole working band.

B. Log-Periodic Array

Log-periodic arrays are wideband antennas built out of resonant (usually narrow-band) elements. Thanks to the log-periodic progression in its geometry, a log-periodic array is suitable to cover a wide bandwidth. Unlike the phased array, the log-periodic topology is able to keep the direction of its beam constant with frequency. The idea behind the log-periodic scaling is that a group of radiating elements covers the radiation in a band, while other groups of radiating elements will radiate similarly at other bands. This way, the active region of a log-periodic array is defined as the elements that will radiate at a given frequency and will constitute a sub-array of sorts. These active regions will have the same radiation properties at different frequencies, so a very stable radiation pattern over frequency can be obtained. The active region of the log-periodic array will perform in a similar way to a phased array. This way, the antenna directivity will be determined by the number of elements that are radiating at a given frequency. To obtain a more stable radiation pattern over the frequency band, an array factor with backfire radiation is desired. To do this, the elements must be placed close to each other. However, if the elements are placed too close, the mutual coupling effect may interfere with the proper behavior of the array, as already noted in [4].

The use of a broadly matched radiating element with a high-pass radiation efficiency adds some particularities to the design of the log-periodic array. Most of them were already covered in [4]. For instance, when the radiating elements have a narrow impedance bandwidth, it is indispensable to add a frequency-constant 180° phase shift between adjacent elements. This way, the mismatch produced by each element when they are not radiating is cancelled out by destructive interference. When a broadly matched element is used, this is not necessary. Furthermore, each element will radiate in a wider band and, for this reason, there is more flexibility in the difference of size between one element and the next. This allows several elements to radiate at once, increasing the directivity of the array. However, if many elements radiate at the same frequency and their sizes and spacing are very different between them, a non-stable array factor over frequency or ripples will be obtained. Additionally, when using the unidirectional radiating element instead of the classic complementary strip-slot, the challenge of dealing with the cavity appears. Again, it is desired to have a narrow cavity to have flexibility in the spacing between elements. In the case of a log-periodic array, an even narrower cavity is needed because the radiating elements must be closer together to obtain backfire radiation. This type of radiation is desired to obtain a more stable radiation pattern over the frequency band. For this reason, a higher than wider cavity was chosen to build the radiating element. A picture of the manufactured array of 15 elements can be seen in Fig. 7. A problem of placing the radiating element this close together is that the mutual coupling between them can be high. An advantage of using the cavity is that the couplings between the stubs are blocked and, this way, the mutual coupling is considerably reduced. Lastly, to avoid the use of filler material in the cavity, a small step has been made into the aluminum to suspend the substrate, so the cavity is filled with air in this case.

Fig. 8 shows the reflection coefficient of the antenna with a broadband 50 Ω load placed at the second port. The agreement between simulation and measurement is good. From 2.1 to 4.3 GHz, the matching is very good, below -12 dB (VSWR

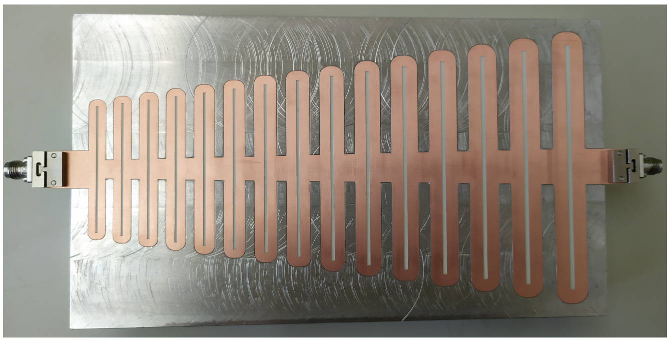

Fig. 7. Picture of the manufactured log-periodic array.

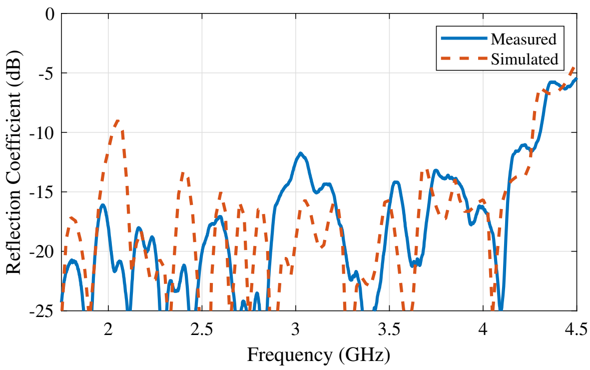

Fig. 8. Reflection coefficient of the proposed log-periodic array.

of 1.7 or lower), an uncommon figure for such a wide bandwidth antenna (over 60% of fractional bandwidth). Note that the bandwidth can be further increased by adding more radiating elements to the array, at the cost of antenna size. Fig. 9 shows the measured and simulated radiation patterns at four different frequencies. The main direction of the beam is around -50° since the array factor has the maximum in the backfire direction and the radiating element has a null in the apex and the maximum at broadside. This combination leads to backward angle radiation. As expected, the shape and direction of the radiation pattern are mostly maintained over frequency. Regardless of this, the maximum directivity of the antenna is considerable, about 10 dBi.

IV. Conclusions

A novel radiating element and two array applications have been analyzed. By closing the structure with a cavity, unidirectional radiation has been obtained. Despite the different behavior of the slot due to the cavity, the use of the complementary stub allows to greatly increase the impedance bandwidth of the radiating element. It can also be modeled with a lattice network. This model has been used to provide physical insight behind the operation principle of the element and to propose a design methodology. Its radiation performance is similar to that of a conventional slot but with unidirectional radiation and a wider bandwidth. The radiating element is suited to build series-fed arrays and so has been demonstrated by the simulation, fabrication, and measurement of two different classic array topologies: a phased array and a log-periodic array. It is expected that its wide bandwidth, excellent radiating properties, and design simplicity make it

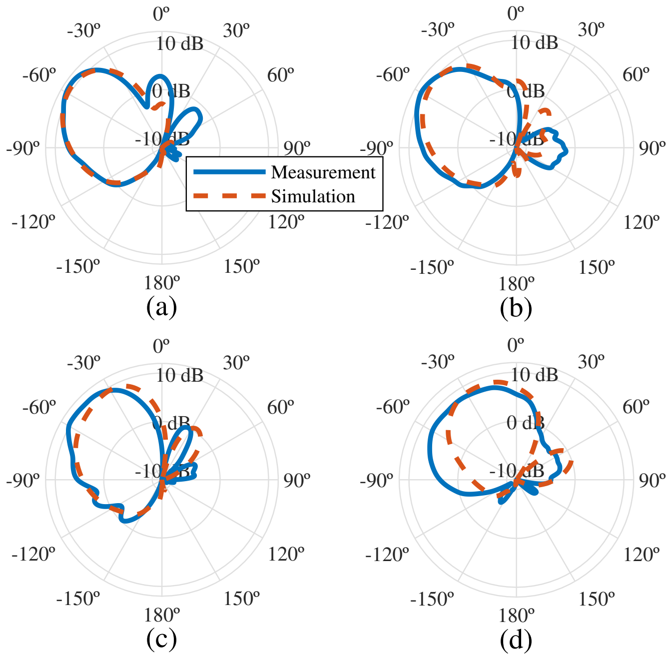

Fig. 9. Radiation patterns of the proposed log-periodic array at different frequencies. (a) 2.25 GHz. (b) 2.75 GHz. (c) 3.5 GHz. (d) 4.25 GHz.

a good candidate for demanding antenna applications.

Acknowledgements

The authors would like to thank Prof. J. Esteban, from Universidad Politécnica de Madrid (Spain), for helping with the measurement of the array and J. M. Romero-Romero for fabricating the 3D-printed material. This work was supported by the Spanish Ministerio de Educación, Cultura y Deporte (Programa para la Formación del Profesorado Universitario) under grant FPU15/06457, by the Spanish Ministerio de Ciencia, Innovación y Universidades (MCIU) (Contrato Juan de la Cierva-Incorporación) under Grant IJC2018-038440-I, and by the MCIU, AEI, and FEDER (Programa Estatal de I+D+i Orientada a los Retos de la Sociedad) under grant RTI2018-097098-J-I00.

References

[1] D. M. Pozar, "Reciprocity method of analysis for printed slot and slot-coupled microstrip antennas," *IEEE Transactions on Antennas and Propagation*, vol. 34, pp. 1439–1446, Dec. 1986.

[2] E. Abdo-Sánchez, J. Page, T. Martín-Guerrero, J. Esteban, and C. Camacho-Peñalosa, "Planar broadband slot radiating element based on microstrip-slot coupling for series-fed arrays," *IEEE Transactions on Antennas and Propagation*, vol. 60, no. 2, pp. 6037–6042, Dec. 2012.

[3] E. Abdo-Sánchez, T. M. Martín-Guerrero, J. Esteban, and C. Camacho-Peñalosa, "Short dual-band planar leaky-wave antenna with broadside effect mitigation," *IET Microwaves, Antennas and Propagation*, vol. 10, no. 5, pp. 574–578, May 2016.

[4] E. Abdo-Sánchez, J. Esteban, T. Martín-Guerrero, and C. Camacho-Peñalosa, "A novel planar log-periodic array based on the wideband complementary strip-slot element," *IEEE Transactions on Antennas and Propagation*, vol. 62, no. 11, pp. 5572–5580, Nov. 2014.

[5] A. Hernández-Escobar, E. Abdo-Sánchez, and C. Camacho-Peñalosa, "A broadband cavity-backed slot radiating element in transmission configuration," *IEEE Transactions on Antennas and Propagation*, vol. 66, no. 12, pp. 7389–7394, Dec. 2018.

[6] M. E. VanValkenburg, *Introduction to Modern Network Synthesis*. Wiley, 1960.

[7] A. Hernández-Escobar, E. Abdo-Sánchez, and C. Camacho-Peñalosa, "A wideband equivalent circuit for stripline-fed cavity-backed slot radiating elements," *IEEE Access*, vol. 7, pp. 166 428–166 434, 2020.